An unusual amino acid substitution within the hummingbird cytochrome *c* oxidase alters a key proton-conducting channel

Cory D. Dunn [a] * and Vivek Sharma [a,b] *

[a] Institute of Biotechnology
Helsinki Institute of Life Science
University of Helsinki
00014 Helsinki
Finland

[b] Department of Physics
University of Helsinki
00014 Helsinki
Finland

* Co-Corresponding Authorship

Cory Dunn, Ph.D.
P.O. Box 56
University of Helsinki
00014 Finland
Email: cory.dunn@helsinki.fi
Phone: +358 50 311 9307

Vivek Sharma, Ph.D.
P.O. Box 64
University of Helsinki
00014 Finland
Email: vivek.sharma@helsinki.fi
Phone: +358 50 5759 509

ABSTRACT

Hummingbirds in flight exhibit the highest metabolic rate of all vertebrates. The bioenergetic requirements associated with hovering flight raise the possibility of positive selection upon proteins encoded by hummingbird mitochondrial DNA. Here, we have identified a non-conservative change within the mitochondria-encoded cytochrome c oxidase subunit I (COI) that is fixed within hummingbirds, yet exceedingly rare among other metazoans. This unusual change can also be identified in several nectarivorous hovering insects, hinting at convergent evolution linked to diet or mode of flight. We performed atomistic molecular dynamics simulations using bovine and hummingbird models, and our findings suggest that COI amino acid position 153 provides genetic control of D-channel hydration and activity. We discuss potential phenotypic outcomes for the hummingbird that are linked to this intriguing instance of positive selection upon the mitochondrial genome.

INTRODUCTION

Hummingbirds are distinguished by their use of hovering flight to feed upon nectar and insects, to defend their territories, and to carry out courtship displays (1–3). Their exceptional mobility demands a prodigious level of mitochondrial ATP synthesis, and indeed, the metabolic rate of hummingbird flight muscles is exceedingly high (4, 5). Many physiological and cellular features of hummingbirds appear to be tailored to their extreme metabolism, especially when considering that hummingbirds can be found within hypoxic environments up to 5000 meters above sea level (6). For example, hemoglobin structure (7) and cellular myoglobin concentration (8) appear to be adapted to the oxygen delivery needs of hummingbirds. Additionally, the hearts of hummingbirds are larger, relative to their body size, than other birds and can pump at a rate of more than 1000 beats per minute (9). Beyond ATP synthesis, the metabolism of these tiny endotherms must also buffer against heat loss (4, 10, 11). At the subcellular level, adaptation to the need for increased ATP and heat production can be readily visualized, since mitochondria in hummingbird flight muscles are highly, perhaps maximally, packed with cristae and are found in close apposition to capillaries (12, 13). Hummingbirds have an exceptionally long lifespan when considering the allometric link between body mass and longevity (14), but whether hummingbird lifespan is linked to its unusual metabolic prowess is unclear.

Within the mitochondrial inner membrane, electrons progress through the electron transport chain (ETC), reach the cytochrome *c* oxidase (COX) complex, and are then used to reduce oxygen. Proton movements coupled to electron passage through COX contribute to the proton motive force (PMF) used for ATP production and thermogenesis (15, 16). While several COX subunits are nucleus-encoded and imported to mitochondria, the core, catalytic subunits of COX (subunits COI, COII, and COIII) are encoded by mitochondrial DNA (mtDNA) (17), raising the possibility that positive selection upon the mitochondrial genome may have contributed to the remarkable metabolic

properties of hummingbirds. Here, we identify an amino acid substitution in COI that is universal among hummingbirds, yet exceedingly rare among other birds and vertebrates. Atomistic molecular dynamics (MD) simulations suggest that this substitution affects COX behavior and is likely to contribute to the uncommon physiological capabilities of hummingbirds.

RESULTS AND DISCUSSION

Hummingbird harbors unusual substitutions within the mitochondria-encoded subunit I of cytochrome c oxidase

We sought coding changes within mtDNA-encoded genes that might license or kindle the extreme metabolic capabilities of hummingbirds. Toward this goal, we analyzed bird mtDNA-encoded protein sequences obtained from the NCBI Reference Sequence (RefSeq) database (18). Upon close inspection of protein sequence alignments, we discovered a surprising substitution of serine for alanine at position 153 of COI in all 15 hummingbird species that were examined (Table S1) (for convenience, we use the number sequence associated with the structurally characterized *Bos taurus* COI subunit). This change was found in no other birds within our alignment of 645 Aves COI entries (Figure 1). Since COI is the most commonly used DNA sequence barcode for studying animal ecology and speciation (19, 20), we next analyzed additional sequences covering the COI region of interest that we obtained from the Barcode of Life Data (BOLD) server (21). Initially, we focused upon sequences from the bird order Apodiformes, which encompasses hummingbirds and swifts. 914 of 915 informative samples annotated as hummingbird-derived were found to carry an A153S substitution at position 153 of COI (Table S2). The remaining sample is mis-annotated as hummingbird, as determined by barcode BLASTN (22) analysis. In contrast, all 110 non-hummingbird Apodiformes samples harbored the ancestral A153. Extending our analysis to all informative bird barcodes, only 15/36,636 samples (< 0.1%) not annotated as hummingbird or its parental clade were divergent at position 153. Assuming that these COI alterations were not the result of sequencing errors, identified changes were not fixed within each identified genus (Table S3).

COI is among the most slowly evolving mtDNA-encoded proteins, with apparently severe limitations on alterations that might be accommodated within this enzyme (23–26). In the high-resolution (1.5 Å) crystal structure (27) of COX from *Bos taurus* (> 87% identical in COI amino acid sequence to hummingbird), amino acid 153 is buried in the middle of COI transmembrane helix IV and is sandwiched between a water-filled cavity lined with polar residues and the D-channel, which is thought to conduct protons for oxygen reduction and generation of the PMF within COX of mitochondria and some bacteria (28, 29) (Figure 2A). Moreover, residue 153 is only 10 Å from the critical E242 that is suggested to control proton movement at the terminus of the D-channel (Figure 2A). No other COI change appears universally encoded by hummingbird mtDNA, and position 153 does not contact a nucleus-

encoded subunit, suggesting the lack of a single compensatory change that would lead to substitution neutrality (30). Since A153 is almost universal among birds, yet appears to be substituted for serine in all hummingbirds, the A153S change within hummingbird COI is likely to have functional relevance and to have been positively selected.

Beyond birds, substitution at A153 was also extremely unusual among chordates, a phylum encompassing vertebrates. Of 4,998 aligned Chordata sequences from the RefSeq dataset, only four non-hummingbird entries suggested a possible change at position 153 (Table S4). Two RefSeq entries, from the sawtooth eel (*Serrivomer sector*) and the kuhli loach (*Pangio cf. anguillaris*), contain the A153S substitution characteristic of hummingbirds. However, further analysis of accumulated COI barcodes suggested that any substitution at position 153 is not widely shared among members of these vertebrate genera, in contrast to members of the hummingbird family, for which the A153S substitution appears universal. Extending our analysis to metazoans, substitution at A153 remains very rare. Indeed, only 146/7942 (< 2%) of informative RefSeq COI sequences harbor a substitution of alanine with any other amino acid at position 153 (Table S5).

Within the class Aves, an additional COI variant appears highly restricted to, but not universal among, hummingbirds. Among the 15 hummingbird COI sequences found within the RefSeq database, nine contained a conservative V83I substitution that is found in no other bird entry (Table S1). Expanding our analysis to Apodiformes barcodes obtained from BOLD, 110/110 non-hummingbird samples carried the V83 allele ancestral for birds. In contrast, 671/929 informative hummingbird samples within this dataset carried a V83I substitution, and 258/929 samples harbored a valine at this position (Table S2). Looking more broadly at 36,878 bird samples, substitution at V83 is very rare among birds (< 0.1%), although unlike the A153S substitution, V83I may be widely shared among members of several non-hummingbird genera (Table S3). Interestingly, it appears that a V83I substitution occurred early in the evolution of hummingbirds and is ancestral for this clade, then subsequently reverted to valine several times during hummingbird expansion (Figure S1). An analysis of BOLD entries performed blind to hummingbird species and to details of sample acquisition suggests that hummingbirds encoding V83 or I83 can be found within overlapping geographical regions, yet there is a trend toward recovery of hummingbirds carrying the I83 allele at higher altitudes (Figure S2 and Table S6). Within the COX enzyme, amino acid 83 lies within 9 Å of COI residue D91, which contributes to proton uptake via the eponymous D-channel described above (Figure 2A). Position 83 is also located within 6 Å of N80, a component of the 'asparagine gate' which is thought to move protons toward the active site (31–33).

Evidence for convergent evolution toward a polar amino acid substitution at position 153 of cytochrome c oxidase subunit I

During our analysis of metazoan COI, our attention was drawn to the prominent presence of A153S, and the similar non-conservative

substitution A153T, in several bee species. Bees and hummingbirds are nectarivorous, thermogenic, and take advantage of energetically expensive hovering flight (1, 34). Moreover, bee metabolic rate relative to mass surpasses even that of hummingbird (35). Analysis of BOLD samples from hymenopteran families Apidae and Megachilidae, the "long-tongued" bees (36), indicate nearly 100% substitution at COI position 153 to either serine or threonine, while other families of bees harbor an ancestral alanine at position 153 (Table S7). Curiously, examination of COI sequences from millions of insect samples found in BOLD indicated that A153S and A153T conversion characterizes many, but not all genera within the Eristalini tribe of dipteran hoverfly (Table S8). Hoverflies within this clade very closely mimic bees visually and behaviorally (37). Together, our results hint at the exciting possibility of convergent evolution, potentially rooted in diet and foraging behavior, at the mitochondria-encoded COI.

Atomistic molecular dynamic simulations suggest that substitution at COI amino acid 153 has functional consequences for proton transport

In an attempt to understand the functional relevance of the A153S change that is common to all hummingbirds, we performed atomistic classical MD simulations on two different vertebrate model systems at differing scales. Remarkably, multiple microsecond simulations demonstrated changes in hydration within the vicinity of position 153 that were coupled to the dynamics of the aforementioned E242, a residue central to redox-coupled proton pumping by COX (15, 16). Specifically, during simulations of the entire 13-subunit wild-type bovine COX performed in membrane-solvent environment, E242 was typically found in the 'down' state ($\chi 2 \sim 60^{\circ}$), extending towards the D-channel proton uptake site D91 (Figures 2B and 2D). In contrast, upon A153S substitution, the bovine E242 commonly swung to the 'up' position ($\chi 2 \sim 180^{\circ}$, Figures 2C and 2D). Similar findings emerged (Figures 2E-G) from longer simulations performed on small bovine model systems, suggesting that the observed behavior is robust. The microscopic changes in hydration near E242 stabilized its 'up' position (Figures 2C and 2F), resulting in water pathways connecting COI regions near the positively charged intermembrane space (Figures S3). During simulations using a constructed hummingbird homology model, we saw that E242 behavior and channel hydration was dependent upon whether alanine or serine was present at position 153 (Figure 2H-I), although the effect was less prominent than in bovine models. In the constructed hummingbird model containing its wild-type S153 variant, E242 was stabilized in the 'down' position. Upon S153A replacement, both 'up' and 'down' populations were observed, and increased motility was visualized (Figure 2J) with corresponding changes to local hydration (Figure 2I).

Furthermore, our simulations suggest that the behavior of additional amino acids beyond E242 are affected by the amino acid found at position 153. For example, our hummingbird simulation strongly indicated that a change in F238 side chain angle is linked to E242 motion (Figure S4) and is influenced by whether residue

153 is an alanine or a serine. These data are supported by a GREMLIN co-evolution analysis (38), initiated by analysis of the bovine COI (Table S9), that suggested co-evolutionary coupling between F238 and E242. The behavior of another amino acid, F63, also appeared to depend upon the amino acid occupying position 153 (Figure S5A), stabilizing in the 'down' ($\chi1 \sim -160^\circ$) conformation in large bovine (Figure S5B), small bovine (Figure S5C), and small hummingbird (Figure S5D) A153 models. The 'up' conformation ($\chi1 \sim -77^\circ$) of F63 preferred in all models simulating S153 led to transient influx of water molecules in the domain above residue 153, in agreement with bovine COX structural data (Figures 2A and S5A). Taken together, MD analysis of naturally occurring variants, as performed here with a hummingbird COI variant, clearly provides the opportunity to confirm or refute evolutionary and structural coupling between different regions of COI.

F238 has been suggested to play a key role in oxygen diffusion through COX (39), and indeed hummingbirds are characterized by a profound oxygen consumption rate during flight (4, 5). Therefore, altered behavior of F238 upon A153S substitution prompted us to consider the possibility that oxygen access to COX is augmented in the hummingbird. However, we argue against a scenario in which improved oxygen access is prompted by A153S substitution. First, with caveats related to the evolutionary divergence between bacteria and vertebrates, a S153A substitution in bacterial COI (bacterial A-family cytochrome *c* oxidases harbor an S within their catalytic subunit) led to similar cytochrome *c* oxidation rates and initial proton pumping rates (40, 41). Moreover, the oxygen consumption rate of isolated hummingbird mitochondria, when normalized to mitochondrial inner membrane area, does not notably differ from mammalian mitochondria (12), suggesting similarity in the maximum rate of COX catalysis. Finally, despite any possible stretching of the oxygen channel linked to F238 movement, the access of oxygen to the active site is likely to be hampered by a corresponding 'up' flip of E242 and its surrounding hydration (Figure S4).

What is the phenotypic outcome of the A153S substitution for hummingbirds?

Our results show clear changes to the behavior of key D-channel residues and to surrounding hydration when comparing different COI models harboring alanine or serine at position 153. However, what is the specific positively-selected outcome linked to COI S153 within the hummingbird? Previous experiments using bacteria suggest that amino acid 153 can influence coupling between electron transport and COX proton pumping, indicating that proton motility is a focus of selection during evolution of hummingbirds. Specifically, a serine to aspartic acid change made at the analogous amino acid position in *Rhodobacter sphaeroides* COI abolished proton pumping while allowing electron transport coupled to proton transfer from the periplasmic side of the bacterial inner membrane when the enzyme was analyzed under zero PMF conditions (40, 42). Further suggesting strong selection on proton handling by hummingbird COX, the hummingbird-ancestral V83I substitution that we identified is located near the

'asparagine gate' at the matrix side of the mitochondrial inner membrane, and mutations near this site lead to oxygen reduction without efficient proton pumping (41). Interestingly, coupling has been demonstrated (43) between the asparagine gate and the key E242 residue, the behavior of which is clearly affected by A153S mutation.

Taken together, our computational analyses suggest that positive selection upon hummingbird COI led to altered proton movement near the D-channel. We suggest two potential outcomes of the non-conservative A153S change. First, if the bovine models accurately reflect the outcome of the A153S change, hydration differences associated with the presence of a polar residue at position 153 may promote intrinsic uncoupling (44) of COX when the PMF is high across the mitochondrial inner membrane, even leading to the use of protons from the intermembrane space for oxygen reduction under conditions of high polarization (45). Rapid, on-site decoupling of proton pumping from electron transport may serve as a local response to cessation of flight, when an immediate rise in matrix ATP might lead to excessive PMF, ETC over-reduction, and reactive oxygen species (ROS) production (46, 47). Intrinsic, local, and immediate uncoupling might be particularly important within hummingbird muscle, where the densely packed ETC components could generate a destructive wave of ROS linked to inner membrane hyperpolarization.

Furthermore, hummingbirds require robust thermoregulation, since these organisms have high surface to mass ratios, can be found at elevations associated with low temperatures, and are subject to convective heat loss while engaged in hovering flight (3, 6, 48). Beyond the possibility of heat generation by COX 'slip', or decoupling of electron transport from proton pumping (49), results from our bovine models raise the possibility that changes to COI hydration accompanying A153S substitution might allow direct, albeit limited movement of protons across the inner membrane that could contribute to non-shivering thermogenesis under conditions of high PMF. Our findings regarding the altitudes at which the I83 COI variant can be found are also consistent with a role for D-channel alteration in hummingbird heat generation. Interestingly, thermoregulation might have been an initial selective force toward increased metabolic capacity (50) and therefore may have played a particularly prominent role during the evolution of hummingbirds.

While amino acid substitution at position 153 clearly affects COI hydration and behavior, the phenotypic outcomes outlined above are still somewhat speculative. Models examining the effects of the hummingbird A153S substitution within the well-characterized, yet non-native bovine structure may lead to inaccuracies in predicting COI behavior. Moreover, *in silico* modeling of amino acid substitutions within a constructed COI model that is not built upon the foundation of a high-resolution hummingbird COX structure may not fully recapitulate the actual behavior of hummingbird COI, and indeed our simulations using the hummingbird model provide more equivocal results regarding E242 behavior and nearby hydration. Thus far, the vertebrate mitochondrial genome remains

refractory to directed modification toward a desired sequence change (51), preventing a direct test of the hummingbird-enriched COI substitutions in the background of a related non-hummingbird mtDNA. However, future biochemical experiments guided by our combined use of phylogenetic analysis and atomistic simulations may be informative regarding the role of hummingbird COI changes that have emerged from positive selection, once thought unlikely to shape mitochondria-encoded genes (52). Excitingly, other changes to mtDNA-encoded oxidative phosphorylation machinery beyond the A153S substitution are rare among birds yet common in hummingbirds, and these substitutions await further analysis. Finally, while mtDNA sequence information is far more prevalent for birds, we expect that accumulating nuclear DNA sequence information (53) will allow analysis of divergent nucleus-encoded members of the oxidative phosphorylation machinery and their potential role in hummingbird metabolism.

METHODOLOGY

Sequence acquisition, alignment, and annotation

Available mitochondrial proteomes were downloaded from the NCBI RefSeq database (release 92) (18). Additional COI barcodes were retrieved from the BOLD server (21). Alignments were performed by use of locally installed MAFFT (version 7.407) (54). For much larger, initial alignments of insect COI barcodes, MAFFT was performed using an online server (55, 56). Translations using the appropriate codon table were performed using AliView (74).

Taxonomy analysis was performed using the 'taxize' package (57) and the NCBI Taxonomy database (58), with manual curation when required.

Elevation data matching geolocation latitude and longitude were acquired from the Gpsvisualizer site (www.gpsvisualizer.com).

Modeling and simulation

We constructed small and large model systems of bovine mitochondrial cytochrome *c* oxidase from the high-resolution (1.5 Å) crystal structure (PDB 5B1A) (27). The large model system comprised all thirteen subunits, whereas in the small model only two catalytic subunits (I and II) were included, which allowed us to perform longer timescale simulations. Both wild-type and mutant (A153S) cases were considered. The larger protein system was embedded in a multicomponent lipid bilayer (POPC:POPE:cardiolipin in 5:3:2 ratio) and only single component bilayer (POPC) was used in the case of two subunit complex, both constructed using CHARMM-GUI (59). Solvent water and Na^+ and Cl^- ions (150 mM each) were added. In both setups, metal centers were in oxidized states with a water and an hydroxyl ligand at heme a_3 and Cu_B, respectively. Crosslinked Y244 was anionic [see also (60)]. All amino acids were in their standard protonation states, except E242, K319 and D364 of subunit I, which were kept in a neutral state. The CHARMM force field parameters for protein, water, lipids and metal centers were taken from (61–63). Additional

subunit I/II homology models of hummingbird cytochrome *c* oxidase [both wild-type (S153) and mutant (A153) model systems] were constructed using bovine structure (PDB: 5B1A) and the predicted amino acid sequence of *Florisuga mellivora* (accession YP_009155396.1).

All MD simulations were performed with GROMACS software (64). Prior to production runs, all model systems were subjected to energy minimization followed by an equilibration MD. During equilibration, Nose-Hoover thermostat (65, 66) and Berendsen barostat (67) were applied. LINCS (68) algorithm implemented in GROMACS was applied to achieve the time step of 2 fs. During production runs Nose-Hoover thermostat and Parinello-Rahman barostat (69) were applied to keep temperature and pressure constant at 310 K and 1 atm, respectively. The large and small model systems of bovine oxidase were simulated for 1.5 and 3 μs, respectively. The hummingbird COX wild-type and mutant models were simulated for 1 μs each, resulting in a total of 11 μs of atomistic simulations. VMD (70) was used for the visualization of trajectories and analysis.

ACKNOWLEDGEMENTS

C.D.D. is funded by an ERC Starter Grant (RevMito 637649) and by the Sigrid Jusélius Foundation. V.S. is funded by the Academy of Finland, the University of Helsinki, and the Sigrid Jusélius Foundation. We thank Fyodor Kondrashov for advice on COI sequence recovery and alignment, Gregor Habeck for assistance in use of R Studio, and Aapo Malkamäki for support in MD simulation setup. We also acknowledge the Center for Scientific Computing, Finland for their generous computational support.

AUTHOR CONTRIBUTIONS

C.D.D. performed phylogenetic and taxonomic analyses. V.S. performed molecular dynamics simulations. Both authors prepared the manuscript text and figures.

COMPETING INTERESTS

The authors declare no competing interests.

FIGURE LEGENDS

Figure 1: An alanine to serine substitution at bovine COI position 153 is universal among hummingbirds. Bird orders are arranged based upon a supertree modified from (71) under a Creative Commons license, and results obtained by analysis of RefSeq-acquired protein sequences are reflected.

Figure 2: Hydration-coupled dynamics of conserved residue E242 are altered by the A153S substitution found in hummingbird COI. (A) The D-channel of proton transfer is located near residue 153 (dotted circles) in the high-resolution crystal structure of COX from *Bos taurus* (PDB 5B1A). Crystallographically resolved water molecules (purple spheres) in the domain above A153, together with nearby polar amino acids, form a potential proton transfer path. Cu_B is shown in orange and high spin heme in yellow. The catalytic COI subunit is shown with

transparent ribbons and amino acids are displayed in atom-based coloring. (B-D) COI hydration and E242 side chain position are altered by substitution at COI position 153 in a large bovine COX simulation. (B) illustrates the native structure (A153) and (C) demonstrates the effects of A153S substitution. A red arrow highlights major changes to hydration, and water occupancy is shown as an orange colored mesh at an isovalue of 0.15. (D) E242 side chain dihedral angle (χ2) within COI encoding A153 (black) or S153 (red) during 1.5 μs of bovine large model simulation is displayed. Here, E242 adopts a predominant 'up' conformation within A153S substituted COI. (E-G), as in (B-D), but a small bovine model simulation has been deployed. (H-J), as in (B-D), but a small hummingbird model has been simulated. In (J), S153 (red) is wild-type and A153 (black) is mutant.

SUPPLEMENTARY INFORMATION

Figure S1: COI I83 is ancestral for hummingbirds and reverts to the bird consensus V83 in multiple lineages. Reference mtDNA sequences (release 91) of the indicated organisms were obtained and aligned by MAFFT using the G-INS-i iterative refinement method. Next, a phylogenetic analysis was performed within the MEGA7 software (72) using a maximum likelihood approach based upon the Tamura-Nei model (73). The amino acid at COI position 83 is illustrated next to each organism within the resulting tree.

Figure S2: A meta-analysis suggests that COI I83 may be associated with hummingbird habitation at higher elevation. Violin plots were generated using elevation data listed in Table S5. Median is denoted by the dotted line, with quartiles illustrated by solid black lines.

Figure S3: Water-based paths toward the positively charged intermembrane space. Due to shift in 'down' to 'up' conformation of E242, the side chain of this amino acid connects to the hydrophilic region above heme propionates and near amino acids Y231 and T146 following A153S substitution in a small bovine COI simulation.

Figure S4: The position of the COI F238 side chain is coupled to E242 dynamics. (A) F238 is shown within the hummingbird small model simulation when E242 is in the (A) down position and when E242 points in the (B) up position. F238 dihedral angle (χ1, N-CA-CB-CG) is compared to E242 dihedral angle (χ2, CA-CB-CG-CD) in the (C) bovine big model simulation and in the (D) hummingbird small model simulation. E242 data from Figures 2D and 2J are shown, with F238 dihedral angle for the A153 variant plotted in blue and for the S153 variant plotted in orange.

Figure S5: The dynamic behavior of the conserved F63 is determined by amino acid identity at position 153. (A) Simulation snapshots showing two positions of the F63 sidechain within the bovine COX are shown in green licorice. The 'up' position (χ1 ~ -77°) results in local hydration in the case of A153S substitution mutant, whereas the stable 'down' conformation (χ1 ~ -160°) that blocks the entry of water molecules, is stabilized in wild-type case. The preferred angle of F63 during MD

simulations is altered when alanine is swapped for serine in large (B) and small (C) model system of bovine COX. F63 dynamics are similarly altered in a small model system of hummingbird oxidase (D). A153 (black) and S153 (red).

Table S1: Analysis of full-length bird COI sequences obtained from the RefSeq database. Sequences of all mitochondria-encoded proteins found in the NCBI RefSeq database (release 92) (18) were downloaded, and the COI FASTA sequences of 645 birds were extracted. MAFFT (version 7.407) alignment was performed (54) using the G-INS-i iterative refinement approach, and those birds with a A153S substitution are listed along with the variant harbored by each species at COI position 83.

Table S2: Examination of amino acids 83 and 153 in Apodiformes barcodes obtained from BOLD. The query "Apodiformes" was made using the BOLD server (21) to recover COI FASTA sequences. MAFFT alignment was carried out using L-INS-i iterative refinement method and translated in AliView (74) using the vertebrate mtDNA translation table. Informative samples with annotated species names were assessed to determine the amino acids found at positions 83 and 153.

Table S3: Analysis of Aves COI barcodes obtained from BOLD. The query "Aves" was made using the BOLD server (21) to recover COI FASTA sequences. MAFFT alignment was carried out under the "auto" setting and translated in AliView (74) using the vertebrate mtDNA translation table. Informative COI samples outside of the order Apodiformes and not harboring alanine at position 153 or valine at position 83 are listed.

Table S4: Geolocation data for COI variants found at position 83. For each BOLD accession associated with a hummingbird species, an elevation was derived from Gpsvisualizer. Elevations provided by BOLD (21) were not utilized, since they typically did not match with the BOLD-annotated longitude and latitude and were sparse within the dataset.

Table S5: Analysis of chordate COI sequences obtained from the RefSeq database. COI sequences obtained from the RefSeq database (18) were filtered for chordate entries. MAFFT alignment was performed using the "auto" setting and poorly aligned sequences were deleted. Hummingbird sequences were removed. Four informative, non-hummingbird sequences were characterized by substitution of A153 for other amino acids, although analysis of annotated BOLD accessions labelled with a species name or entry suggest that these COI substitutions are not generally shared throughout each genus.

Table S6: Analysis of metazoan COI sequences obtained from the RefSeq database. COI sequences obtained from the RefSeq database (18) were filtered for metazoan entries. Analysis was performed as in Table S5, and non-chordate samples with a substitution at A153 are displayed.

Table S7: Analysis of bee COI barcodes obtained from BOLD. Entries for bee families Apidae, Megachilidae, Colletidae, Halictidae, Andrenidae, and Melittidae, as defined in (75), were obtained from BOLD (21), but no samples from the small bee family Stenotritidae were available. In addition, no Spheciformes samples were found in BOLD. After deletion of samples not of the COI-5P class or not associated with a species, MAFFT alignment was carried out under the "auto" setting. DNA sequences were translated to the informative reading frame in AliView (74) using the invertebrate mtDNA translation table. Substitution quantification for each family is provided, along with the variant found at position 153 in each sample.

Table S8: Analysis of COI barcodes from Eristalini tribe of hoverflies obtained from BOLD. Entries for the Anasimyia, Eristalinus, Eristalis, Helophilus, Lejops, Mesembrius, Palpada, Parhelophilus, Phytomia, Senaspis, Mallota, Chasmomma genera were obtained and analyzed as in Table S7.

Table S9: GREMLIN analysis of co-evolution. GREMLIN (38) was run using the default settings and the bovine COI sequence as a query.

REFERENCES

1. Norberg UM (1996) Energetics of flight. *Avian Energetics and Nutritional Ecology*, ed Carey C (Chapman & Hall, New York), pp 199–249.
2. Hainsworth FR, Wolf LL (1972) Power for Hovering Flight in Relation to Body Size in Hummingbirds. *Am Nat* 106(951):589–596.
3. Altshuler DL, Dudley R (2002) The ecological and evolutionary interface of hummingbird flight physiology. *J Exp Biol* 205(Pt 16):2325–36.
4. Lasiewski RC (1963) Oxygen consumption of torpid, resting, active, and flying hummingbirds. *Physiol Zool* 36(2):122–140.
5. Suarez RK, Brown GS, Hochachka PW (1986) Metabolic sources of energy for hummingbird flight. *Am J Physiol* 251(3 Pt 2):R537-42.
6. Projecto-Garcia J, et al. (2013) Repeated elevational transitions in hemoglobin function during the evolution of Andean hummingbirds. *Proc Natl Acad Sci U S A* 110(51):20669–74.
7. Projecto-Garcia J, et al. (2013) Repeated elevational transitions in hemoglobin function during the evolution of Andean hummingbirds. *Proc Natl Acad Sci* 110(51):20669–20674.
8. Johansen K, Berger M, Bicudo JEPW, Ruschi A, de Almeida PJ (1987) Respiratory Properties of Blood and Myoglobin in Hummingbirds. *Physiol Zool* 60(2):269–278.
9. Bishop CM (1997) Heart mass and the maximum cardiac output of birds and mammals: Implications for estimating the maximum aerobic power input of flying animals. *Philos Trans R Soc B Biol Sci* 352(1352):447–456.
10. Suarez RK, Gass CL (2002) Hummingbird foraging and the relation between bioenergetics and behaviour. *Comp Biochem Physiol Part A Mol Integr Physiol*

133(2):335–343.

11. López-Calleja MV, Bozinovic F (1995) Maximum Metabolic Rate, Thermal Insulation and Aerobic Scope in a Small-Sized Chilean Hummingbird (Sephanoides sephanoides). *Auk* 112(4):1034–1036.
12. Suarez RK, Lighton JR, Brown GS, Mathieu-Costello O (1991) Mitochondrial respiration in hummingbird flight muscles. *Proc Natl Acad Sci U S A* 88(11):4870–3.
13. Mathieu-Costello O, Suarez RK, Hochachka PW (1992) Capillary-to-fiber geometry and mitochondrial density in hummingbird flight muscle. *Respir Physiol* 89(1):113–32.
14. Calder III WA (1990) Avian Longevity and Aging. *Genetic Effects on Aging*, ed Harrison DE (Telford Press, West Caldwell, NJ, USA), pp 185–204.
15. Wikström M, Sharma V (2018) Proton pumping by cytochrome c oxidase - A 40 year anniversary. *Biochim Biophys acta Bioenerg* 1859(9):692–698.
16. Wikström M, Krab K, Sharma V (2018) Oxygen Activation and Energy Conservation by Cytochrome c Oxidase. *Chem Rev* 118(5):2469–2490.
17. Johnston IG, Williams BP (2016) Evolutionary inference across eukaryotes identifies specific pressures favoring mitochondrial gene retention. *Cell Syst* 2(2):101–111.
18. O'Leary NA, et al. (2016) Reference sequence (RefSeq) database at NCBI: current status, taxonomic expansion, and functional annotation. *Nucleic Acids Res* 44(D1):D733–D745.
19. Pentinsaari M, Salmela H, Mutanen M, Roslin T (2016) Molecular evolution of a widely-adopted taxonomic marker (COI) across the animal tree of life. *Sci Rep* 6(October):1–12.
20. Hill GE (2015) Mitonuclear Ecology. *Mol Biol Evol* 32(8):1917–27.
21. Ratnasingham S, Hebert PDN (2007) bold: The Barcode of Life Data System (http://www.barcodinglife.org). *Mol Ecol Notes* 7(3):355–364.
22. Altschul SF, Gish W, Miller W, Myers EW, Lipman DJ (1990) Basic local alignment search tool. *J Mol Biol* 215(3):403–10.
23. da Fonseca RR, Johnson WE, O'Brien SJ, Ramos MJ, Antunes A (2008) The adaptive evolution of the mammalian mitochondrial genome. *BMC Genomics* 9:119.
24. Stewart JB, et al. (2008) Strong purifying selection in transmission of mammalian mitochondrial DNA. *PLoS Biol* 6(1):e10.
25. Meiklejohn CD, Montooth KL, Rand DM (2007) Positive and negative selection on the mitochondrial genome. *Trends Genet* 23(6):259–63.
26. Castellana S, Vicario S, Saccone C (2011) Evolutionary patterns of the mitochondrial genome in Metazoa: Exploring the role of mutation and selection in mitochondrial protein-coding genes. *Genome Biol Evol* 3(1):1067–1079.
27. Yano N, et al. (2016) The Mg 2+ -containing Water Cluster of Mammalian Cytochrome c Oxidase Collects Four Pumping Proton Equivalents in Each

Catalytic Cycle. *J Biol Chem* 291(46):23882–23894.

28. Kaila VRI, Sharma V, Wikström M (2011) The identity of the transient proton loading site of the proton-pumping mechanism of cytochrome c oxidase. *Biochim Biophys Acta - Bioenerg* 1807(1):80–84.
29. Wikström M, Verkhovsky MI (2011) The D-channel of cytochrome oxidase: An alternative view. *Biochim Biophys Acta - Bioenerg* 1807(10):1273–1278.
30. Blier PU, Dufresne F, Burton RS (2001) Natural selection and the evolution of mtDNA-encoded peptides: evidence for intergenomic co-adaptation. *Trends Genet* 17(7):400–6.
31. Henry RM, Yu C-H, Rodinger T, Pomès R (2009) Functional Hydration and Conformational Gating of Proton Uptake in Cytochrome c Oxidase. *J Mol Biol* 387(5):1165–1185.
32. Liang R, Swanson JMJ, Wikström M, Voth GA (2017) Understanding the essential proton-pumping kinetic gates and decoupling mutations in cytochrome c oxidase. *Proc Natl Acad Sci* 114(23):5924–5929.
33. Ghane T, et al. (2018) Hydrogen-Bonded Network and Water Dynamics in the D-channel of Cytochrome c Oxidase. *J Membr Biol* 251(3):299–314.
34. Loli D, Bicudo JEPW (2005) Control and regulatory mechanisms associated with thermogenesis in flying insects and birds. *Biosci Rep* 25(3–4):149–80.
35. Suarez RK, Staples JF, Lighton JR, Mathieu-Costello O (2000) Mitochondrial function in flying honeybees (Apis mellifera): respiratory chain enzymes and electron flow from complex III to oxygen. *J Exp Biol* 203(Pt 5):905–11.
36. Cariveau DP, et al. (2016) The Allometry of Bee Proboscis Length and Its Uses in Ecology. *PLoS One* 11(3):e0151482.
37. Golding YC, Edmunds M (2000) Behavioural mimicry of honeybees (Apis mellifera) by droneflies (Diptera: Syrphidae: Eristalis spp.). *Proc R Soc London Ser B Biol Sci* 267(1446):903–909.
38. Kamisetty H, Ovchinnikov S, Baker D (2013) Assessing the utility of coevolution-based residue-residue contact predictions in a sequence- and structure-rich era. *Proc Natl Acad Sci* 110(39):15674–15679.
39. Mahinthichaichan P, Gennis RB, Tajkhorshid E (2018) Cytochrome aa3 Oxygen Reductase Utilizes the Tunnel Observed in the Crystal Structures To Deliver O2 for Catalysis. *Biochemistry* 57(14):2150–2161.
40. Namslauer A, et al. (2007) Plasticity of Proton Pathway Structure and Water Coordination in Cytochrome c Oxidase. *J Biol Chem* 282(20):15148–15158.
41. Pfitzner U, et al. (2000) Tracing the D-Pathway in Reconstituted Site-Directed Mutants of Cytochrome c Oxidase from Paracoccus denitrificans †. *Biochemistry* 39(23):6756–6762.
42. Pawate AS, et al. (2002) A mutation in subunit I of cytochrome oxidase from Rhodobacter sphaeroides results in an increase in steady-state activity but

completely eliminates proton pumping. *Biochemistry* 41(45):13417–23.

43. Vakkasoglu AS, Morgan JE, Han D, Pawate AS, Gennis RB (2006) Mutations which decouple the proton pump of the cytochrome c oxidase from Rhodobacter sphaeroides perturb the environment of glutamate 286. *FEBS Lett* 580(19):4613–4617.
44. Murphy MP, Brand MD (1988) The stoichiometry of charge translocation by cytochrome oxidase and the cytochrome bc1 complex of mitochondria at high membrane potential. *Eur J Biochem* 173(3):645–51.
45. Mills DA, Schmidt B, Hiser C, Westley E, Ferguson-Miller S (2002) Membrane potential-controlled inhibition of cytochrome c oxidase by zinc. *J Biol Chem* 277(17):14894–901.
46. Papa S, Guerrieri F, Capitanio N (1997) A possible role of slips in cytochrome C oxidase in the antioxygen defense system of the cell. *Biosci Rep* 17(1):23–31.
47. Kadenbach B (2003) Intrinsic and extrinsic uncoupling of oxidative phosphorylation. *Biochim Biophys Acta* 1604(2):77–94.
48. Altshuler DL, Dudley R, McGuire JA (2004) Resolution of a paradox: hummingbird flight at high elevation does not come without a cost. *Proc Natl Acad Sci U S A* 101(51):17731–6.
49. Musser SM, Chan SI (1995) Understanding the cytochrome c oxidase proton pump: thermodynamics of redox linkage. *Biophys J* 68(6):2543–2555.
50. Bennett AF (1991) The evolution of activity capacity. *J Exp Biol* 160:1–23.
51. Patananan AN, Wu TH, Chiou PY, Teitell MA (2016) Modifying the Mitochondrial Genome. *Cell Metab* 23(5):785–796.
52. Little AG, Lougheed SC, Moyes CD (2012) Evolution of mitochondrial-encoded cytochrome oxidase subunits in endothermic fish: The importance of taxon-sampling in codon-based models. *Mol Phylogenet Evol* 63(3):679–684.
53. Zhang G (2015) Bird sequencing project takes off. *Nature* 522(7554):34.
54. Katoh K, Standley DM (2013) MAFFT multiple sequence alignment software version 7: improvements in performance and usability. *Mol Biol Evol* 30(4):772–80.
55. Katoh K, Rozewicki J, Yamada KD (2017) MAFFT online service: multiple sequence alignment, interactive sequence choice and visualization. *Brief Bioinform* (June):1–7.
56. Kuraku S, Zmasek CM, Nishimura O, Katoh K (2013) aLeaves facilitates on-demand exploration of metazoan gene family trees on MAFFT sequence alignment server with enhanced interactivity. *Nucleic Acids Res* 41(W1):W22–W28.
57. Chamberlain SA, Szöcs E (2013) taxize: taxonomic search and retrieval in R. *F1000Research* 2:191.
58. Federhen S (2012) The NCBI Taxonomy database. *Nucleic Acids Res* 40(D1):D136–D143.
59. Lee J, et al. (2016) CHARMM-GUI Input Generator for NAMD, GROMACS, AMBER, OpenMM, and CHARMM/OpenMM Simulations Using

the CHARMM36 Additive Force Field. *J Chem Theory Comput* 12(1):405–413.

60. Malkamäki A, Sharma V (2019) Atomistic insights into cardiolipin binding sites of cytochrome c oxidase. *Biochim Biophys Acta - Bioenerg* 1860(3):224–232.
61. Klauda JB, et al. (2010) Update of the CHARMM all-atom additive force field for lipids: validation on six lipid types. *J Phys Chem B* 114(23):7830–43.
62. Best RB, et al. (2012) Optimization of the additive CHARMM all-atom protein force field targeting improved sampling of the backbone φ, ψ and side-chain χ(1) and χ(2) dihedral angles. *J Chem Theory Comput* 8(9):3257–3273.
63. MacKerell AD, et al. (1998) All-atom empirical potential for molecular modeling and dynamics studies of proteins. *J Phys Chem B* 102(18):3586–616.
64. Abraham MJ, et al. (2015) GROMACS: High performance molecular simulations through multi-level parallelism from laptops to supercomputers. *SoftwareX* 1–2:19–25.
65. Nosé S (1984) A unified formulation of the constant temperature molecular dynamics methods. *J Chem Phys* 81(1):511–519.
66. Hoover WG (1985) Canonical dynamics: Equilibrium phase-space distributions. *Phys Rev A* 31(3):1695–1697.
67. Berendsen HJC, Postma JPM, van Gunsteren WF, DiNola A, Haak JR (1984) Molecular dynamics with coupling to an external bath. *J Chem Phys* 81(8):3684–3690.
68. Hess B (2008) P-LINCS: A Parallel Linear Constraint Solver for Molecular Simulation. *J Chem Theory Comput* 4(1):116–122.
69. Parrinello M, Rahman A (1981) Polymorphic transitions in single crystals: A new molecular dynamics method. *J Appl Phys* 52(12):7182–7190.
70. Humphrey W, Dalke A, Schulten K (1996) VMD: Visual molecular dynamics. *J Mol Graph* 14(1):33–38.
71. Davis KE, Page RDM (2014) Reweaving the tapestry: a supertree of birds. *PLoS Curr* 6(506):1–91.
72. Kumar S, Stecher G, Tamura K (2016) MEGA7: Molecular Evolutionary Genetics Analysis Version 7.0 for Bigger Datasets. *Mol Biol Evol* 33(7):1870–4.
73. Tamura K, Nei M (1993) Estimation of the number of nucleotide substitutions in the control region of mitochondrial DNA in humans and chimpanzees. *Mol Biol Evol* 10(3):512–26.
74. Larsson A (2014) AliView: a fast and lightweight alignment viewer and editor for large datasets. *Bioinformatics* 30(22):3276–8.
75. Sann M, et al. (2018) Phylogenomic analysis of Apoidea sheds new light on the sister group of bees. *BMC Evol Biol* 18(1):71.

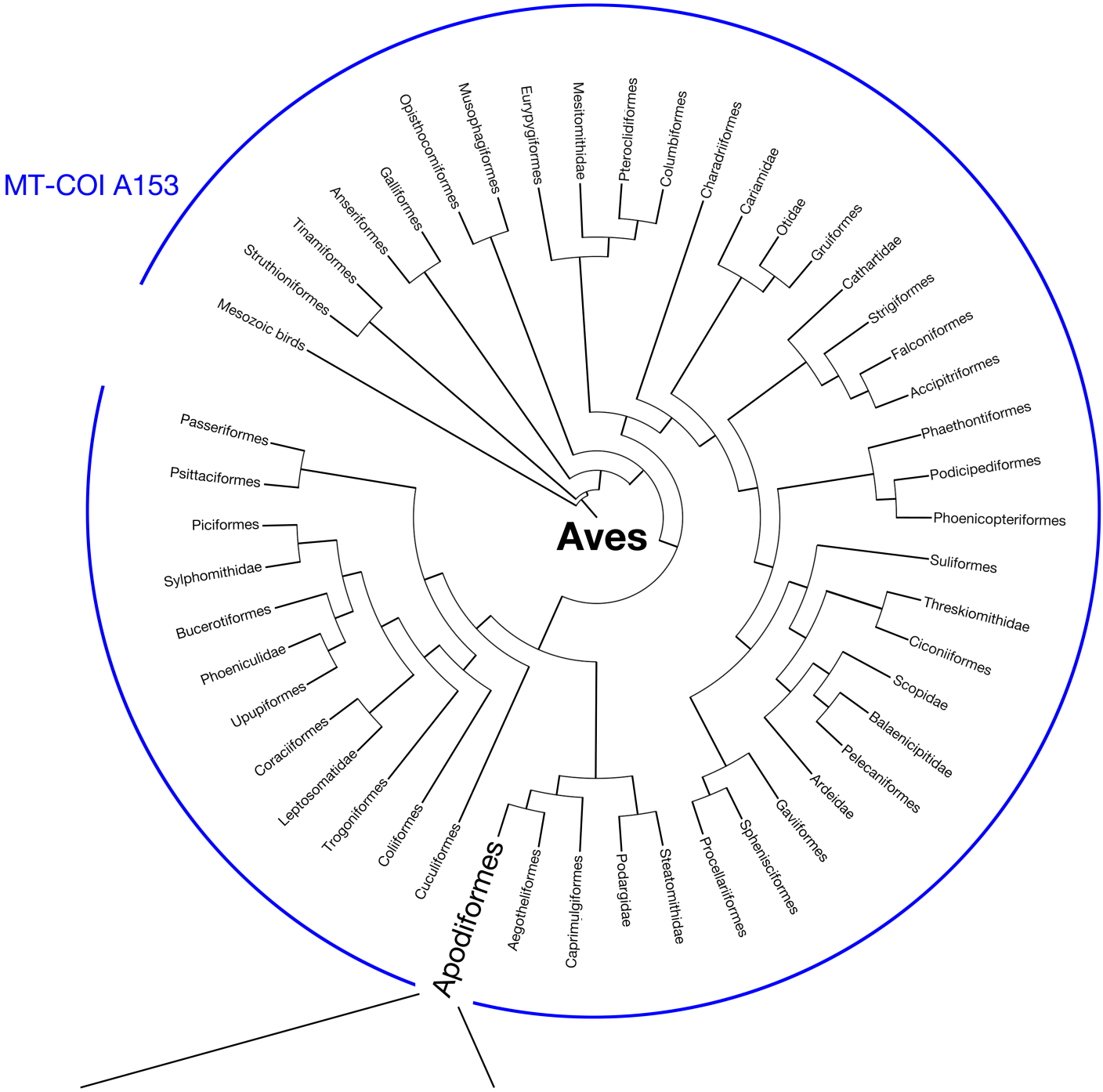

Figure 1

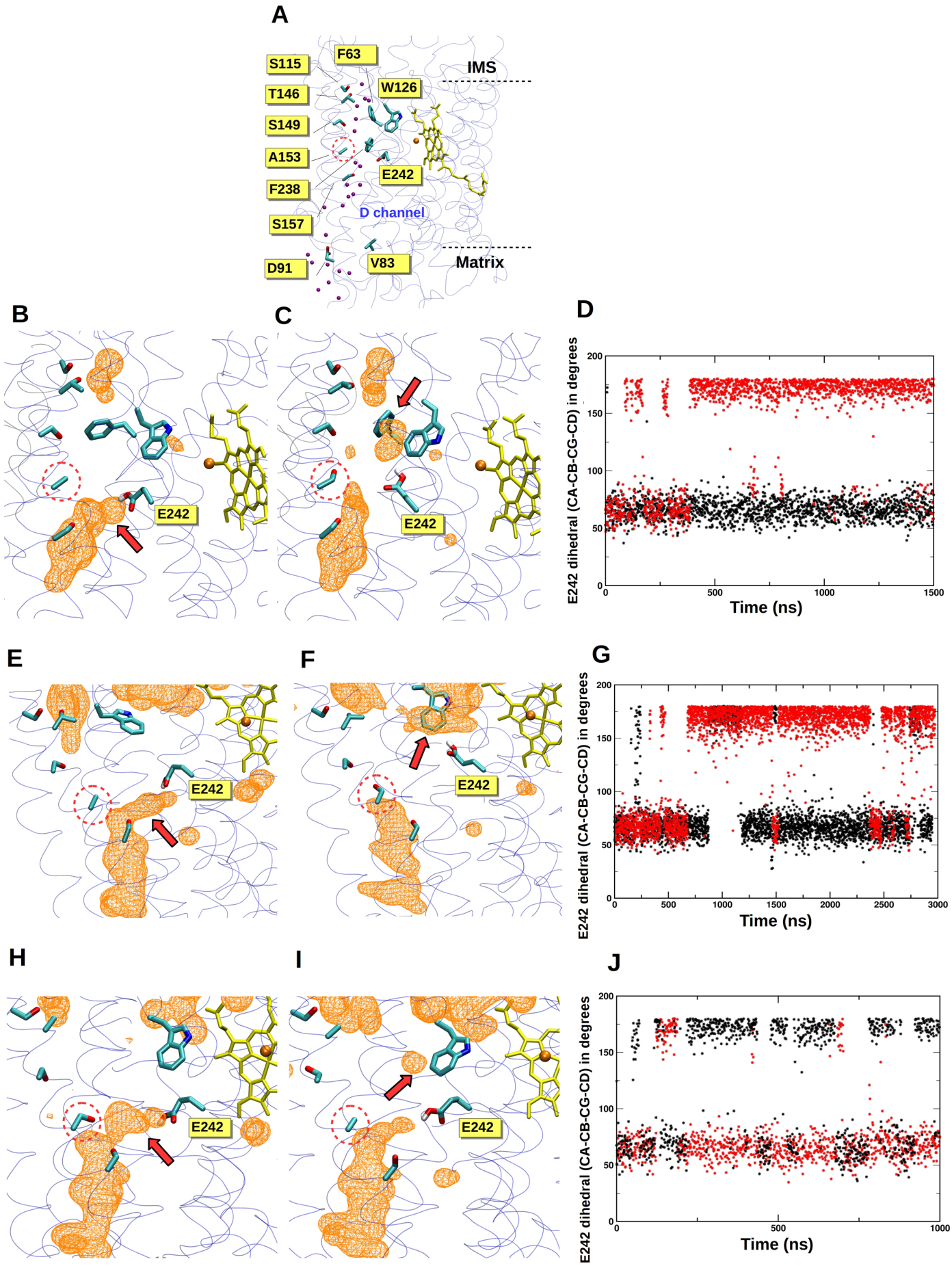

Figure 2